Research Article

SOHAG JOURNAL OF SCIENCES

https://doi.org/10.21608/sjsci.2023.179767.1046

Study of the Effect of Thickness on the Optical Properties of $MnBi_{0.95}Sb_{0.05}$ Thin Film

Esraa Y. Omar*, A. M. Ahmed, A. K. Diab, and H. F. Mohamed

Physics Department, Faculty of Science, Sohag University, Sohag 82524, Egypt.
**E-mail: esraayaseen65@yahoo.com*

Received: 9th December 2022, **Revised:** 20th January 2023, **Accepted:** 22nd January 2023.
Published online: 25th January 2023

Abstract: $MnBi_{0.95}Sb_{0.05}$ alloys were prepared by the conventional melt technique and then deposited as a thin film by thermal evaporation technique with different thicknesses. The optical absorption, reflection, and transmission spectra of thin films were measured in the wavelength range of 250 nm to 2500 nm. In our work, $MnBi_{0.95}Sb_{0.05}$ thin films have a hexagonal structure (P63/mmc group). The optical properties are characterized by high absorption and reflection, as well as very low transmission. Besides that, the absorbance of $MnBi_{0.95}Sb_{0.05}$ films decreased with increasing thickness. The calculated energy gap of $MnBi_{0.95}Sb_{0.05}$ thin films depended on the film thickness. It decreases from 1.36V to 1.03V by increasing the thickness from 25nm to 75nm. Different optical parameters like n, k, and σ_{opt} are examined and discussed.
Keywords: $MnBi_{0.95}Sb_{0.05}$ thin films, thermal evaporation method, optical properties, optical band gap.

1. Introduction

Thin films have recently attracted much interest from researchers due to their practical application in photodetectors, solar cells, and quantum electronics. The thermal evaporation technique is the widest method for producing an amorphous solid in the form of a thin film, in addition to its simplicity. The MnBi-MnSb matrix has been widely studied over the years using both bulk and thin-film samples. MnBi and MnSb are symmetric, with a Ni element having a hexagonal crystal structure. Both MnSb and MnBi have a hexagonal Ni-as-type structure, it has been proposed that a new MnBiSb ternary system with a suitable composition would also form a hexagonal structure **[1]**.

In $Mn_{0.5-}(Bi_{0.25}Sb_{0.75})$ thin film, the hexagonal structure and crystal lattice constant were found to be larger than those of MnBi and MnSb with semiconductor properties [2]. Additionally, it has a high refractive index and absorption coefficient. Gobel et al. **[3]** observed that the presence of a unique ferromagnetic phase with a Ni-as-type structure is only for Sb-rich compounds ($x > 0.7$). The authors note that for all other compositions, the presence of more than one crystalline phase. The crystal structure phases for low doping of Sb ($0.05 \leq x \leq 0.15$) content in the MnBi-MnSb system were studied. In addition, the composition of the crystal structure and differences in optical constants such as energy gap, extinction coefficient (k), refractive index (n), and optical conductivity (σopt) were calculated and discussed.

$MnBi_{1-x}Sb_x$ alloys have significant applications in the thermoelectric industry, and Sb doping has been observed to increase power factor (PF) and figure of merit (ZT) **[4]**. MnBi double thin films have been studied because they are important for magneto-optical (MO) storage media using the Curie laser writing technique **[5]**. In addition, the SbBi alloy film is very important for photonic films in near-field SR (super-resolution) functional film structures [6]. The objective of this work is to study the effect of the thickness on the optical properties of $MnBi_{0.95}Sb_{0.05}$ thin film.

2. Materials and methods

2.1 Sample preparation

The elements Sb (99.9%), Bi (99.99%), and Mn (99.9%) were mixed well with ground after taking the required proportions, then pressed into tablet form and packed into a vacuum quartz ampule. The alloy was synthesized in three stages:

i. The pressed disks were placed in a furnace, where they remained for 24 hours at 813 K, after which the furnace was turned off and left to cool to room temperature.

ii. The ingots are mixed by ground after the first stage of preparation for 30 minutes until homogenized and pressed into a disc at a pressure of 3 ton.cm^{-2}. The disc was placed in a vacuum quartz ampule and heated for 24 hours at 1273 K; then they were quenched in iced water.

iii. $MnBi_{0.95}Sb_{0.05}$ was deposited by thermal evaporation using a coating unit (Manufactured using Technology Licensed from Edwards Ltd, Auto 306). MnBiSb thin film was grown on a glass layer of three different thicknesses.

Evaporation deposition is performed under high vacuum conditions in order to obtain the desired level of purity for the thin films. The digital film thickness monitor model SQM-160 uses a proven INFICON quartz crystal sensor (6 MH- with gold electrodes) was used to measure the film thickness and deposition rate of deposition processes by the well-established crystal microbalance technique.

2.2 Thin film Characterization

The crystal structure was carried out by X-ray diffraction (XRD) using Brucker (Axs-D&Advace) powder diffractometer at room temperature with Cu(K_α) radiation (λ=1.5406 Å) and under ambient temperature conditions. The microstructure and morphology of MBSb thin films were performed by scanning electron microscopy (SEM Model JSM IT200). Optical transmission and reflection spectra were measured at room temperature using UV/Vis absorption (JASCO V570) spectrophotometer over the wavelength 200-2500nm. In the case of R measurement, an additional attachment model ISN - 470 is provided. The measured T and R values of the deposited Mn $Bi_{0.95}$ $Sb_{0.05}$ film were used to determine numerous optical constants, such as extinction index (k), refractive index (n), and absorption coefficient (α).

3. Results and Discussion

3.1 Crystal structure

Fig. 1 shows the XRD pattern of 25&75-nm-thick $MnBi_{0.95}Sb_{0.05}$ thin film. It was found that all peaks belong to Bi, Mn, Mn_2Sb, MnBi, and Mn-Bi-Sb phases. The $MnBi_{0.95}Sb_{0.05}$ phase has manifested at 2θ = 27.3, 39.6, 48.9, and 56.4 °, while the Bi and Mn_2Sb phases only appeared at a peak at 2θ = 22.5 and 38.19° respectively. These data are in good agreement with previous studies [4]. The highest peak of (0 0 2) Mn–Bi–Sb phase with a hexagonal Ni-as-type structure is detected in the $MnBi_{0.95}Sb_{0.05}$ film, presenting that some Mn–Bi–Sb nanocrystals are oriented using the c-axis perpendicular to the film surface [7]. Therefore, the crystal structure of the ternary phase can be described with the formation of Mn-Bi-Sb as a p63/mmc hexagonal group, which was subsequently confirmed by Gabay et al. [8]. As the second phase Mn_2Sb associated with the tetragonal P4/n mm (129) [9] and the allied hexagonal bismuth phase R-3m (166) [8-10]. Fig. 2 shows the scanning electron microscopy of a 75-nm-thick $MnBi_{0.95}Sb_{0.05}$ thin film. It can be seen that a uniform distribution of grain sizes is found, and they correlated well with each other. Slight porosity is observed.

3.2 Optical Properties

Fig. 3 shows the absorbance of thin films of $MnBi_{0.95}Sb_{0.05}$ as a function of the wavelength at different thicknesses (25 nm, 50 nm, and 75 nm). It observed a very high value of absorbance at 50nm thickness, and the absorbance increases and decreases with increasing the wavelength. Fig. 4 shows the absorption coefficient (α) spectra at different thicknesses of $MnBi_{0.95}Sb_{0.05}$ thin film. It can be seen that the absorption coefficient decreases with increasing thickness. Fig. 5 shows the reflectance spectra of $MnBi_{0.95}Sb_{0.05}$ thin films deposited at different thicknesses. It can be seen that the reflectance is low in the region (300 - 600 nm) and high in the near-infrared region for all thicknesses. (Fig. 6) shows transmittance spectra of thin films deposited at different thicknesses. The transmittance decreases with increasing thickness and reaches nearly zero at higher thicknesses. In the ultra-thin film (25nm) the reflectance and transmittance are less than 25% with the absorbance to be achieved above 75% in the 400-1000 nm wavelength region as matching the solar radiation spectrum [11].

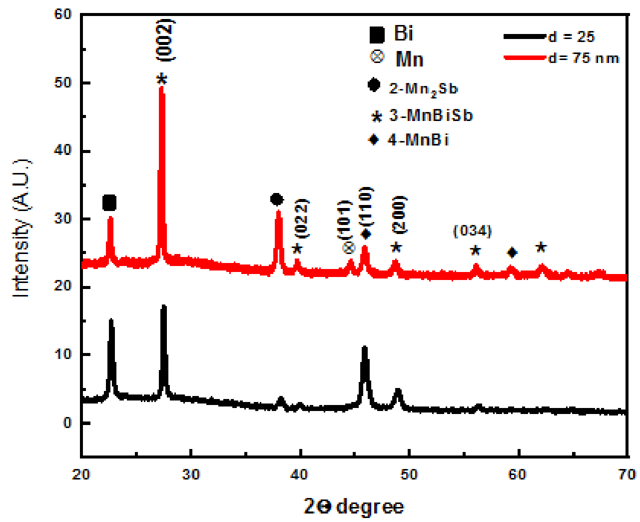

Fig. 1. XRD pattern of 25&75-nm-thick $MnBi_{0.95}Sb_{0.05}$ thin film.

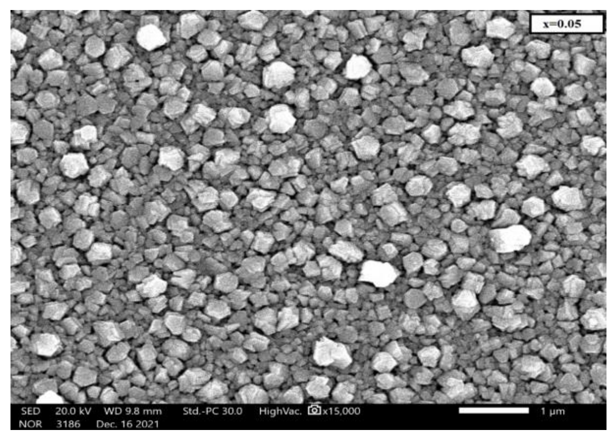

Fig. 2. The scanning electron microscopy of MnBi0.95Sb0.05 with a thickness 75nm.

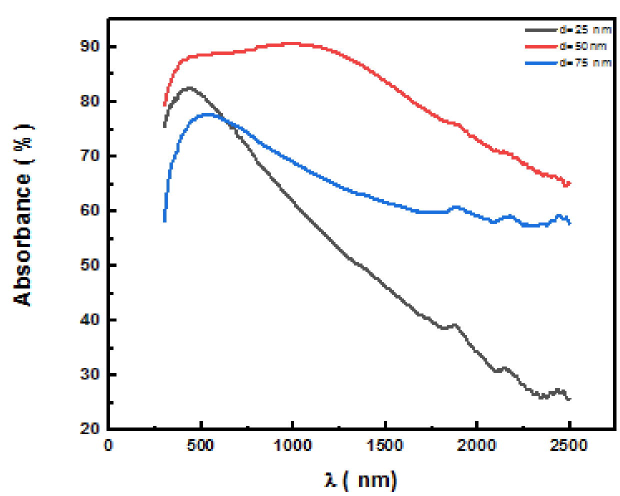

Fig. 3. Absorbance spectra of $MnBi_{0.95}Sb_{0.05}$ thin film deposited at different thicknesses.

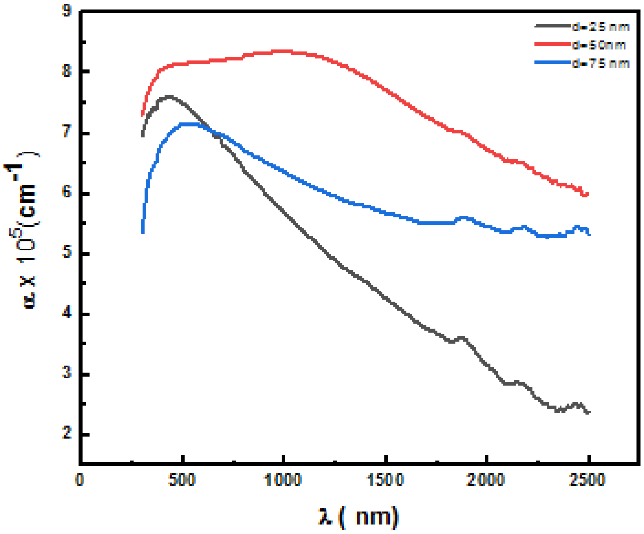

Fig. 4. The absorption coefficient (α) sepctra at different thicknesses of $MnBi_{0.95}Sb_{0.05}$ thin film.

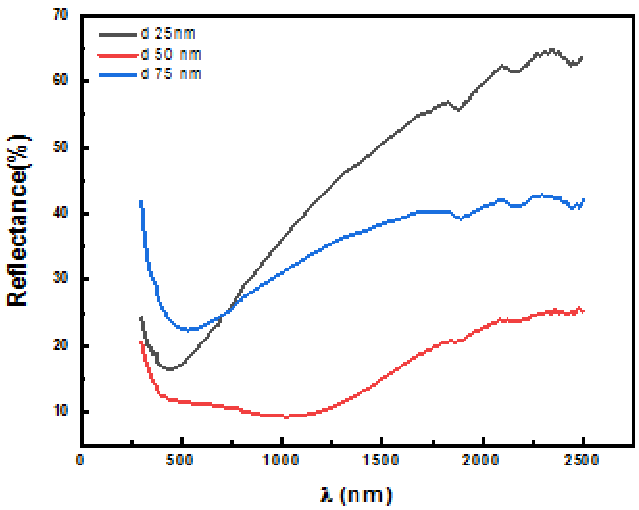

Fig. 5. Reflectance spectra of $MnBi_{0.95}Sb_{0.05}$ thin films deposited at different thicknesses.

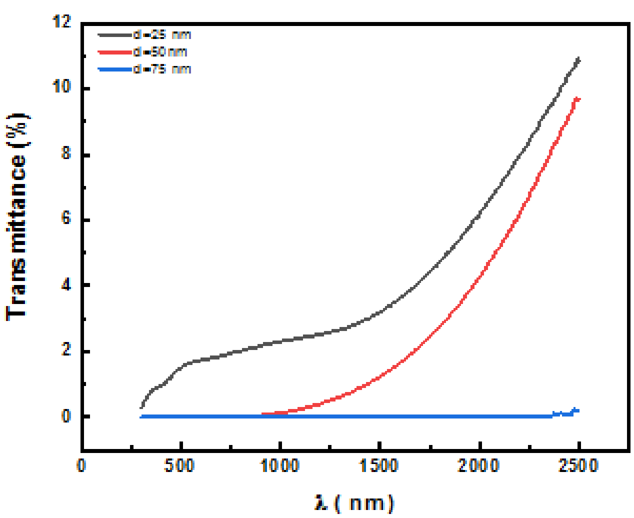

Fig. 6. Transmittance spectra of $MnBi_{0.95}Sb_{0.05}$ thin films deposited at different thicknesses.

3.3 Optical band gap

The optical bandgap (E_g) of the $MnBi_{0.95}Sb_{0.05}$ films could be calculated from the optical absorption spectra (A). In particular, α of the films depends on the optical absorbance and the film thickness, where α was determined from the following equation:

$$(\alpha) = 2.303\ A / t \qquad (2)$$

where (A) is absorbance and (t) is the thickness of the thin film. It is known that, according to Tauc theory, semiconductors like $MnBi_{0.95}Sb_{0.05}$ are regarded as direct bandgap semiconductors, where α depends on the photon energy (hν) of optical absorption near the band edge in semiconductors which is applied by the following equation [12-15].

$$(\alpha h\nu)^{1/n} = C(h\nu - E_g) \qquad (3)$$

where E_g is the optical bandgap, A is a constant, and n = ½ is for an allowed direct type of transition [16, 17]. The E_g values were estimated by extrapolating the linear portion of the intercept to the energy axis (Fig. 7). The calculated energy gap of $MnBi_{0.95}Sb_{0.05}$ thin film decreased from 1.36 eV to 1.03 eV with increasing thickness, as shown in (Table 1). Obviously, the bandgap varies linearly with the inverse square of the thickness ($1/t^2$), So the quantum size effect is probably the reason for the change in the optical band gap.

The effect of the thickness on the optical band gap can be interpreted as the following: As the thickness of the thin film increases, the transmittance usually decreases and shifts to higher wavelengths, thus the optical absorption edge shifts towards the higher wavelengths, and as a result, the optical gap energy decreases. Sandomirskii [18] was the first to suggest that when the thickness of a thin film is of the order of the de Broglie wavelength of conduction electrons and much lower than the mean free path of charge carriers, the material exhibits a quantum-size effect. The energy component along the thickness is quantized and given by [18 - 20].

$$\nabla E = \frac{h^2}{8m^* \times t^2} \qquad (4)$$

where m^* is the effective mass of the charge carrier, t is the film thickness, h is Planck's constant, and ΔE is the energy component along the thickness. The lowest states of the valence band edge and the conduction band edge are shifted to the lowest non-zero state, causing the band gap to decrease as a function of the inverse square thickness. Above, it was found that, the effect of the quantum size is dominant (explaining the dependence of the band gap on the film thickness) and not the effect due to the difference in dislocation intensity [21]

3.4 The refractive index and Extinction coefficient (n, k)

The refractive index (n) relates to the amount of light absorption, and the extinction coefficient (k) relates to the light absorption frequency. The determination of refractive index indices is very important, especially for these materials that can be used to make any optical device such as switches, filters, modulators, etc.

The refractive index of this thin film is calculated as:

$$n = \frac{(1+R)^{0.5}}{(1-R)^{0.5}} \quad (5)$$

Table 1: Values of E_g verses $1/t^2$ for $MnBi_{0.95}Sb_{0.05}$ thin film.

Thickness	E_g (eV)	$1/t^2$ $(nm)^{-2}$
25 nm	1.36	0.0016
50 nm	1.17	0.0004
75 nm	1.03	0.0002

The extinction coefficient (k) for the film was calculated using the relationship

$$K = \frac{\alpha\lambda}{4\pi} \quad (6)$$

where α is the absorption coefficient

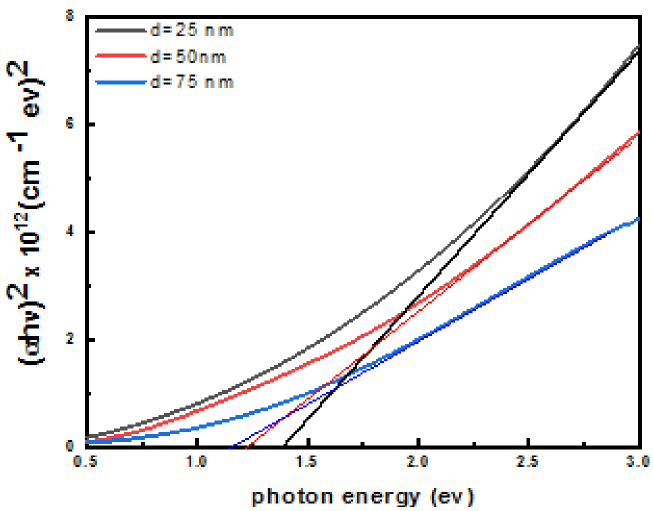

Fig. **7.** The optical band gap (E_g) of $MnBi_{0.95}Sb_{0.05}$ thin film deposited at different thicknesses.

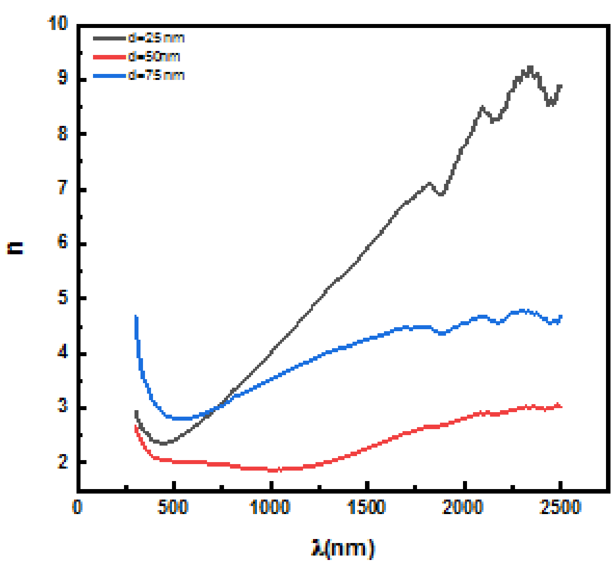

Fig. **8.** The refractive index (n) of $MnBi_{0.95}Sb_{0.05}$ thin films deposited at different thicknesses

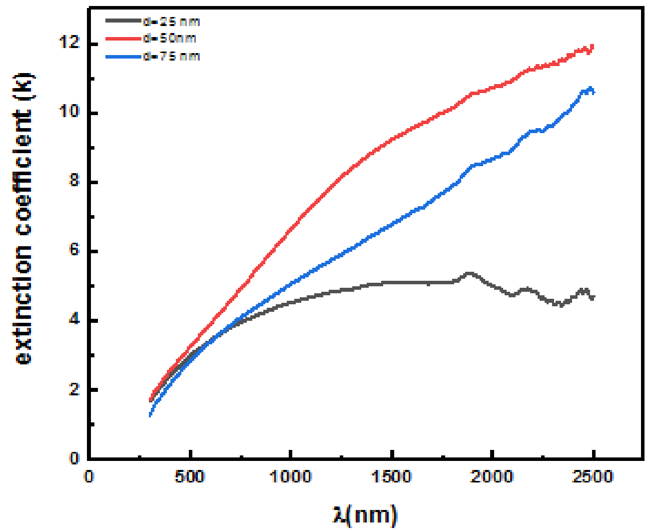

Fig. **9.** The extinction coefficient (k) of $MnBi_{0.95}Sb_{0.05}$ thin films deposited at different thicknesses.

As in (Figs **8 and 9**), the refractive index of $MnBi_{0.95}Sb_{0.05}$ thin film decreases and then increases. Besides, The extinction coefficient (K) of $MnBi_{0.95}Sb_{0.05}$ thin film increases with increasing wavelength, and it decreases with increasing thickness. This is a result of reducing the absorption coefficient by increasing the thickness.

3.5 The optical conductivity

The optical conductivity (σ_{opt}) is estimated using absorption coefficient (α) as follows

$$\sigma_{opt} = \frac{\alpha n c}{4\pi} \quad (7)$$

Where c is the velocity of light.

The optical conductivity σ_{opt}, decreases and then increases with increasing photon energy (Fig. **10**). In addition, it changes unsequenced with increasing thickness. The increase in optical conductivity can be attributed to the increase in absorption coefficient and also may be due to the electron excited by photon energy [22].

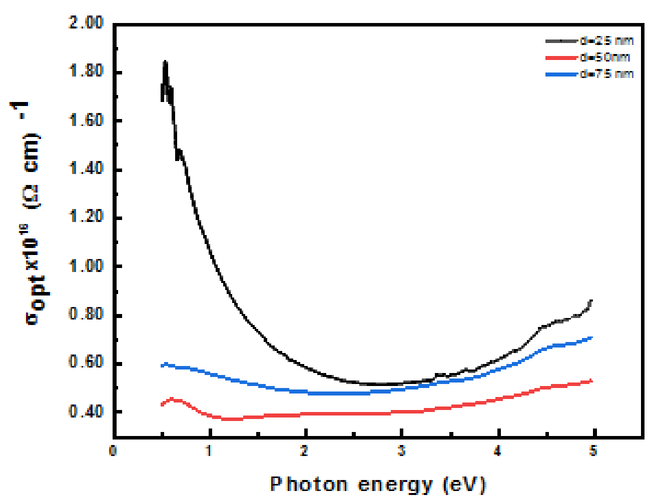

Fig. **10.** Optical conductivity (σ_{opt}) vs. photon energy of $MnBi_{0.95}Sb_{0.05}$ thin films deposited at different thicknesses.

4. Conclusion

The effect of thickness on the structural and optical properties of $MnBi_{0.95}Sb_{0.05}$ thin film fabricated by the thermal evaporation technique was studied. The highest peak of (0 0 2) Mn–Bi–Sb phase with a hexagonal Ni-as-type structure is detected in the $MnBi_{0.9}5Sb_{0.05}$ film. Therefore, the crystal structure of the ternary phase with the formation of Mn-Bi-Sb as a p63/mmc hexagonal group. It was found that the absorbance of $MnBi_{0.95}Sb_{0.05}$ films decreased with increasing thickness. Optical band gap values were found to decrease with thickness from 1.36 to 1.03 eV. Various optical parameters such as n, k, and opt are studied and discussed.

References

[1] K. Kang, V.G. Kravets, A.K. Petford-Long, *Thin solid films*, 410 (2002) 28-37.
[2] Y.J. Wang, J. X. Shen, Q. Tang, *Journal of magnetism and magnetic materials* 74 (1988) 365-369.
[3] H. Göbel, E. Wolfgang, H. Harms, *Physica status solidi*, 34(2) (1976) 553-564.
[4] A.M. Ahmed, H.F. Mohamed, A.K. Diab, E.Y. Omar, *Inf. Sci. Lett.* 12(1) (2023) 149-157.
[5] G.C. Hadjipanayis, R.W. Siegel (Eds.), *Nanophase Materials*, Kluwer, Netherlands, 1994.
[6] X.M. Lu, Y.Q.Wu, Y. Wang, *In Materials Science Forum*, 663 (2011) 227-230.
[7] G.K. Williamson, W.H. Hall, *Acta metallurgica*, 1 (1953) 22-31.
[8] A.M. Gabay, G. C. Hadjipanayis, J. Cui, *Journal of Alloys and Compounds*, 792 (2019) 77- 86.
[9] W.B. Pearson, *Crystalline Materials*, 171 (1985) 23-40.
[10] P. Cucka, C.S. Barrett, *Acta Crystallographica*, 15 (9) (1962) 865–872.
[11] V. G. Kravets, I.V. Poperenko, *Optical Materials*, 21(4) (2003) 765-774.
[12] P.I. Jacques. *Optical processes in semiconductors Prentice-Hall. New Jersey* 92 (1971) 36.
[13] M.A. Butler, *Journal of Applied Physics* 48(5) (1977) 1914-1920.
[14] K.M. Gadave, C. D. Lokhande, *Thin olid Films* 229(1) (1993) 1-4.
[15] B.M. Celalettin, N. Orhan, *Thin Solid Films 518(*8) (2010) 1925-1928.
[16] M. C Baykul, A .Balcioglu, *Microelectronic Engineering*, 51(2000) 703 -713.
[17] C. Yu-Pin, L. Si-Chen, *Journal of Applied Physics*, 83(8) (1998) 4111-4123.
[18] V.B. Sandomirskii, *Sov. Phys. JETP*, 25(1) (1967) 101.
[19] R.P. Khatri, S.M. Vyas, D. Shah, P.Patel, M.P. Jani, G. R. Pandya, *International Journal of Physics and Applications* 2(3) (2010) 95-99.
[20] M.M. Abd El-Raheem, A.H.M. Solieman, M. M.Wakkad, H.M. Ali, S.K. Mohammed, H.F. Mohamed, *Physica Scripta*, 97(8) (2022) 085807.
[21] R. P. KhatrlI, et al. *International Journal of Physics and Applications* 2(3) (2010) 95-99.
[22] F. Yakuphanoglu, A .Cukurovali , I .Yilmaz, *Opt. Mater*. 27 (2005) 1363-1368.